Clays and Clay Minerals, Vol. 60, No. 3, 227–239, 2012.

INFLUENCE OF SYNTHESIS CONDITIONS ON THE FORMATION OF A KAOLINITE-METHANOL COMPLEX AND SIMULATION OF ITS VIBRATIONAL SPECTRA

JAKUB MATUSIK[1,*], EVA SCHOLTZOVÁ[2], AND DANIEL TUNEGA[2,3]

[1] Department of Mineralogy, Petrography and Geochemistry, Faculty of Geology, Geophysics and Environmental Protection, AGH University of Science and Technology, al. Mickiewicza 30, 30-059 Krakow, Poland
[2] Institute of Inorganic Chemistry, Slovak Academy of Sciences, Dúbravská Cesta 9, SK-845 36 Bratislava, Slovak Republic
[3] Institut für Bodenforschung, Universität für Bodenkultur, Peter-Jordan-Strasse 82b, A-1190 Vienna, Austria

Abstract—Kaolinite is often used as a base for the synthesis of new organo-mineral nanomaterials designed for applications in industry and in environmental protection. To make the mineral structure more likely to interact with organic molecules, a kaolinite-methanol complex (KM) can be used. In the present study, different experimental procedures were tested to investigate the formation of the KM. The kaolinite-dimethyl sulfoxide intercalation compound (KDS), either wet or dried, was used as a pre-intercalate. The samples obtained were characterized using X-ray diffraction, Fourier-transform infrared spectroscopy, CHNS elemental analysis, ^{13}C CP-magic angle spinning nuclear magnetic resonance (MAS NMR), and ^{27}Al and ^{29}Si MAS NMR techniques. The method of density functional theory with dispersion corrections (DFT-D2) was used to explain the structure and to simulate the vibrational spectra of KM. Theoretical results were compared with experimental data. The most effective formation of the KM (d_{001} = 11.1 Å − wet; d_{001} = 8.7 Å − dried) was observed when the dried KDS precursor was used. In such conditions the degree of intercalation reached ~98% after 24 h of reaction time. As indicated by the CHNS elemental analysis, ~⅙ of the inner-surface OH groups were grafted by OCH_3 groups. The esterification reaction was less efficient at higher temperatures or when wet KDS was used. In the latter case, the excess of very polar dimethyl sulfoxide molecules prevented intercalation of methanol and further grafting. Detailed analysis of the results of theoretical simulations revealed that the reaction of the KDS with methanol led to the formation of kaolinite with both grafted methoxy groups and intercalated methanol, and water molecules in the interlayer space. The spectra calculated revealed the contribution of individual vibrational modes into the complex bands, *i.e*. the energy of C−H vibrations was in the order: $\nu_{as}CH_{met} > \nu_{as}CH_{mtx} > \nu_{s}CH_{met} > \nu_{s}CH_{mtx}$.

Key Words—DFT-D2, Grafting, Intercalation, Kaolinite, Methanol, Vibrational Spectra.

INTRODUCTION

Kaolinite is a layered 1:1 dioctahedral aluminum silicate with the chemical composition $Al_2Si_2O_5(OH)_4$. Kaolinite layers consist of linked tetrahedral and octahedral sheets where the octahedral side is terminated by inner-surface hydroxyl groups of a μ-OH type. Although the layers are held together *via* hydrogen bonds, kaolinite can be intercalated with various molecules relatively easily (Wada, 1961; Johnston and Stone, 1990; Franco and Ruiz Cruz, 2004; Li *et al.*, 2009). The intercalation process opens access to the basal surfaces, which can be modified by further treatment. The interlayer aluminol groups are susceptible to grafting with different organic molecules (Tunney and Detellier, 1993; Itagaki and Kuroda, 2003; Murakami, 2004; Gardolinski and Lagaly, 2005; Letaief and Detellier, 2007; Avila *et al.*, 2010; Hirsemann *et al.*, 2011, Moretti *et al.*, 2012). As kaolinite is one of the most abundant clay minerals and is available relatively cheaply, much attention is focused on it as a suitable material for obtaining new grafted materials with novel properties and functionalities in comparison to the parent materials (Tonle *et al.*, 2007; Letaief *et al.*, 2008; de Faria *et al.*, 2009; Matusik *et al.*, 2009; Kuroda *et al.*, 2011; Matusik *et al.*, 2011a, Machado *et al.*, 2012). Grafting of aluminol surfaces with methanol can lead to modification of the hydrophillicity/hydrophobicity of clay surfaces (Tunney and Detellier, 1996; Komori *et al.*, 2000). Therefore, the kaolinite-methanol complex (KM) is an interesting material which may be used successfully as a precursor for obtaining, for example, kaolinite-amine derivatives and kaolinite-polymer nanocomposites (Komori *et al.*, 1999; Kuroda *et al.*, 2011; Matusik *et al.*, 2011b, 2012).

As yet, the most efficient synthesis procedure and the structure of the KM are still not known completely and further study is required. Tunney and Detellier (1996) showed that the grafting takes place at an elevated temperature and pressure. Mild conditions at room temperature were shown to be efficient (Komori *et al.*, 2000). The following questions arise. What are the optimum synthesis conditions? Is the complex which is formed an intercalate or a grafted compound? Does the new structure contain water molecules? In a study of complex systems, combining experiment with molecular

* E-mail address of corresponding author:
jakub_matusik@wp.pl
DOI: 10.1346/CCMN.2012.0600301

modeling is a good approach to obtain a detailed understanding. Molecular modeling is also very useful in interpretation of the experimental results. In the present study, the experimental study of methoxy-kaolinite complexes was combined with a theoretical approach based on density functional theory (DFT). Numerous DFT-based studies of structure and properties of kaolinite and some kaolinite intercalates have been reported, *e.g.* a detailed study of hydrogen bonding and OH-stretching frequencies in kaolinite and dickite was performed by Benco *et al.* (2001a, 2001b, 2001c) using a DFT approach combined with molecular dynamics. A cluster-model approach and a B3LYP/3-21G method was used in the study of intercalates and surface adsorbates of kaolinite and dickite with formamide (FA), N-methylformamide (NMFA), and dimethyl sulfoxide (DMSO) by Michalková *et al.* (2002). The DMSO-kaolinite intercalate, with various degrees of intercalation, was investigated by means of a DFT approach and periodic structural models (Michalková and Tunega, 2007). The stability and mutual orientations of molecules in FA- and NMFA-kaolinite intercalates were studied theoretically by Scholtzová *et al.* (2008). The hydrogen bonds and complete vibrational spectra analysis of kaolinite intercalated with DMSO and dimethylselenoxide was presented by Scholtzová and Smrčok (2009). A computational study of the reaction path for the formation of a grafted methoxy group during the oxidation of methanol to formaldehyde by N_2O on the $[Fe]^{1+}$-ZSM-5 cluster using B3LYP/6-31G(d,p) was published by Fellah (2011).

The objective of the present study was to investigate experimentally and theoretically the influence of the synthesis conditions on the formation and structure of the KM. Quantum mechanical (DFT) calculations were performed to characterize bonding of the grafted surface with the adjacent layer. Vibrational spectra were also calculated with a view to analyzing and interpreting the experimental IR spectra. As layers in kaolinite are kept together by hydrogen bonds and because, in the case of surfaces grafted by methoxy groups, the importance of weak dispersion interactions increases, the calculations were performed at the DFT-D2 level where corrections for dispersion interactions are included in accordance with suggestions by Grimme *et al.* (2007).

MATERIALS AND METHODS

Materials

The <40 μm, well ordered kaolinite (M40) from the Maria III deposit (Poland) was used in the present study. The structural and textural characterization of the starting material has been described elsewhere (Matusik *et al.*, 2009, 2011a). The DMSO and methanol were obtained from POCH (Polish Chemical Reagents).

Synthesis of complexes

The Maria III kaolinite intercalated with DMSO (M40DS) was prepared according to a procedure described previously (Olejnik *et al.*, 1968; Matusik *et al.*, 2011a). This material was used as a precursor of grafted kaolinite. Five different experimental procedures (E1−E5) were tested (Table 1). The wet M40DS was reacted with methanol at: 50ºC (E1) or 20ºC (room temperature) (E2−E5). Samples were collected after 15 min (E1), 30 min (E2, E3), and 24 h (E4, E5), and were characterized using X-ray diffraction (XRD), Fourier-transform infrared spectroscopy (FTIR), and CHNS elemental analyses were performed for samples dried at 120ºC. In E1 and E2 the methanol was not changed during the experiment. For E3−E5, the suspensions were centrifuged and dispersed in a fresh portion of methanol after each sample collection. In E5, dried M40DS rather than wet (as in E1−E4) was treated as in E4.

Analytical methods

Powder XRD patterns were recorded using a Philips APD PW 3020 X'Pert instrument (Almelo, Netherlands) with CuKα radiation and a graphite monochromator. Samples were analyzed in the range 2−30º2θ with a step size of 0.05º2θ. The samples were recorded either with or without drying as specified above. Each sample was covered with a foil when recorded, without drying, to prevent evaporation of the methanol. The degree of intercalation (ID) was calculated according to the following formula:

$$ID = I_{11}/(I_{11}+I_7)*100\% \quad (1)$$

where I_{11} is the intensity of the basal spacing reflection of the new complex, I_7 is the intensity of a basal-spacing

Table 1. Summary of the experimental conditions.

	Experiment				
	E1	E2	E3	E4	E5
Precursor	Wet M40DS	Wet M40DS	Wet M40DS	Wet M40DS	Dried M40DS
Temperature (ºC)	50	20	20	20	20
Methanol changes[a]	–	–	+	+	+
Sample collection interval	15 min	30 min	30 min	24 h	24 h

[a] Sample dispersed in fresh methanol after each sample collection: yes (+), no (–)

reflection of kaolinite. The FTIR spectra were collected using a Nicolet 380 spectrometer (Thermo Scientific, Waltham, Massachusetts, USA) from standard KBr pellets (1 mg of sample/200 mg of KBr) with 64 scans at 4 cm^{-1} resolution in the 4000–400 cm^{-1} mid-IR region. Elemental analysis was performed using a VarioEL III Elementar CHNS analyzer (Hanau, Germany).

Solid-state ^{13}C CP-MAS NMR spectra were recorded on the 500 MHz Bruker Avance III spectrometer (Billerica, Massachussets, USA) at 12 kHz. The resonance frequency was 125.775 MHz, and a cross-polarization (CP) pulse sequence was applied with the 2 ms contact time. Tetramethylsilane (TMS) was used as a reference. The ^{29}Si and ^{27}Al solid state MAS-NMR spectra were measured on the APOLLO console (Tecmag, Houston, Texas, USA) at the magnetic field of 7.05 T produced by the 300 MHz/89 mm superconducting magnet (Magnex). The spinning speed was 8 kHz for the ^{27}Al measurements (resonance frequency = 59.515 MHz) and 4 kHz for the ^{29}Si measurements (resonance frequency = 78.068 MHz). The frequency scale (ppm) was referenced to $Al(NO_3)_3$ and TMS for the ^{27}Al and ^{29}Si measurements, respectively.

Computational methods

All calculations were performed using the *Vienna Ab Initio Simulation Package*, *VASP* (Kresse and Furthmüller, 1996a, 1996b) which is based on DFT. The parameterization of the local exchange-correlation function according to Perdew and Zunger (1981), together with a generalized gradient approximation (GGA) for non-local corrections (Perdew and Wang, 1992), was used. The Kohn-Sham equations were solved variationally with a plane-wave (PW) basis set using an energy cutoff of 500 eV in the projector-augmented-wave (PAW) method (Blöchl, 1994; Kresse and Joubert, 1999) in four *k*-point sampling of the Brillouin zone. The optimization procedure was based on a conjugate-gradient algorithm with a stopping criterion of 10^{-7} eV for the total energy, and of 0.001 eV/Å for the root mean square force. No symmetry restrictions were applied during any relaxation procedure.

Because of anisotropy of the structure of clay minerals (especially in the *c* direction) and weak interactions between layers, all DFT calculations were performed by means of a DFT-D2 approach where dispersion corrections were added (Grimme *et al.*, 2007).

Computational models

The structural model of pure kaolinite was constructed on the basis of the structural data published by Neder *et al.* (1999). The starting cell parameters were: a = 5.154 Å, b = 8.942 Å, c = 7.401 Å, α = 91.69º, β = 104.61º, and γ = 89.82º. A summary formula of the model was $Al_4Si_4O_{10}(OH)_8$. Four structural models of the kaolinite complexes with methanol were constructed for the computational study. These models reflected several possible interactions of kaolinite with methanol including intercalated and/or grafted structures. The first model (Figure 1a) represented a kaolinite intercalated with methanol (K-INT) and was based on the atomic coordinates of the kaolinite intercalated with DMSO, taken from the study of Raupach *et al.* (1987). The starting computational cell contained two molecules of methanol in the interlayer space and its summary formula was $Al_4Si_4O_{10}(OH)_8(CH_3OH)_2$. The second model (Figure 1b) represented kaolinite with one grafted methoxy group (K-MTX). Here, one OH inner-surface group was substituted by one methoxy group and the summary formula of this model was $Al_4Si_4O_{10}(OH)_7(CH_3O)$. The third model (Figure 1c) represented a mixed state, where one grafted methoxy group and one intercalated methanol molecule were present (K-MIX). In the fourth K-MIXW model, one water molecule was added into the interlayer space of the K-MIX model (Figure 1d). All structural models were constructed in an attempt to explain the experimental observations.

RESULTS AND DISCUSSION

Experiments 1–4 (wet M40DS)

A significant shift of the kaolinite d_{001} reflection from 7.2 Å to 11.2 Å in the XRD patterns confirmed the formation of an intercalate with DMSO (M40DS) (Figure 2). The second- and third-order reflections of the complex were also found at 5.62 Å and 3.73 Å, respectively. Their presence indicated a significant stacking order of kaolinite layers along the *c* axis. The ID calculated according to equation 1 for the M40DS sample was 98.2%. In the experimental conditions applied, no greater ID values were possible.

The IR spectrum of pure kaolinite revealed the presence of four distinct bands in the OH-stretching region which are characteristic of a highly ordered kaolinite (Figure 3). The bands at 3697, 3670, and 3653 cm^{-1} were attributed to inner-surface OH groups with the band at 3621 cm^{-1} attributed to inner OH groups located between octahedral and tetrahedral sheets (Ledoux and White, 1964; Farmer and Russell, 1967; Johnston and Stone, 1990; Bougeard *et al.*, 2000). After intercalation of DMSO, significant changes took place in the OH-stretching region (Figure 3), in agreement with earlier studies (Olejnik *et al.*, 1968; Frost *et al.*, 2000). The new bands observed at 3539 and 3504 cm^{-1} were connected to hydrogen bonding between DMSO and the kaolinite octahedral surface (Olejnik *et al.*, 1968; Scholtzová and Smrčok, 2009). The signals attributed to C–H stretching modes of DMSO methyl groups were observed at 3023 and 2936 cm^{-1}. Two resonances (43.9 and 42.8 ppm) in the ^{13}C CP-MAS NMR spectrum of the M40DS (Figure 4) were identical to those reported previously (Duer *et al.*, 1992; Hayashi, 1997) and indicated two different local environments for the

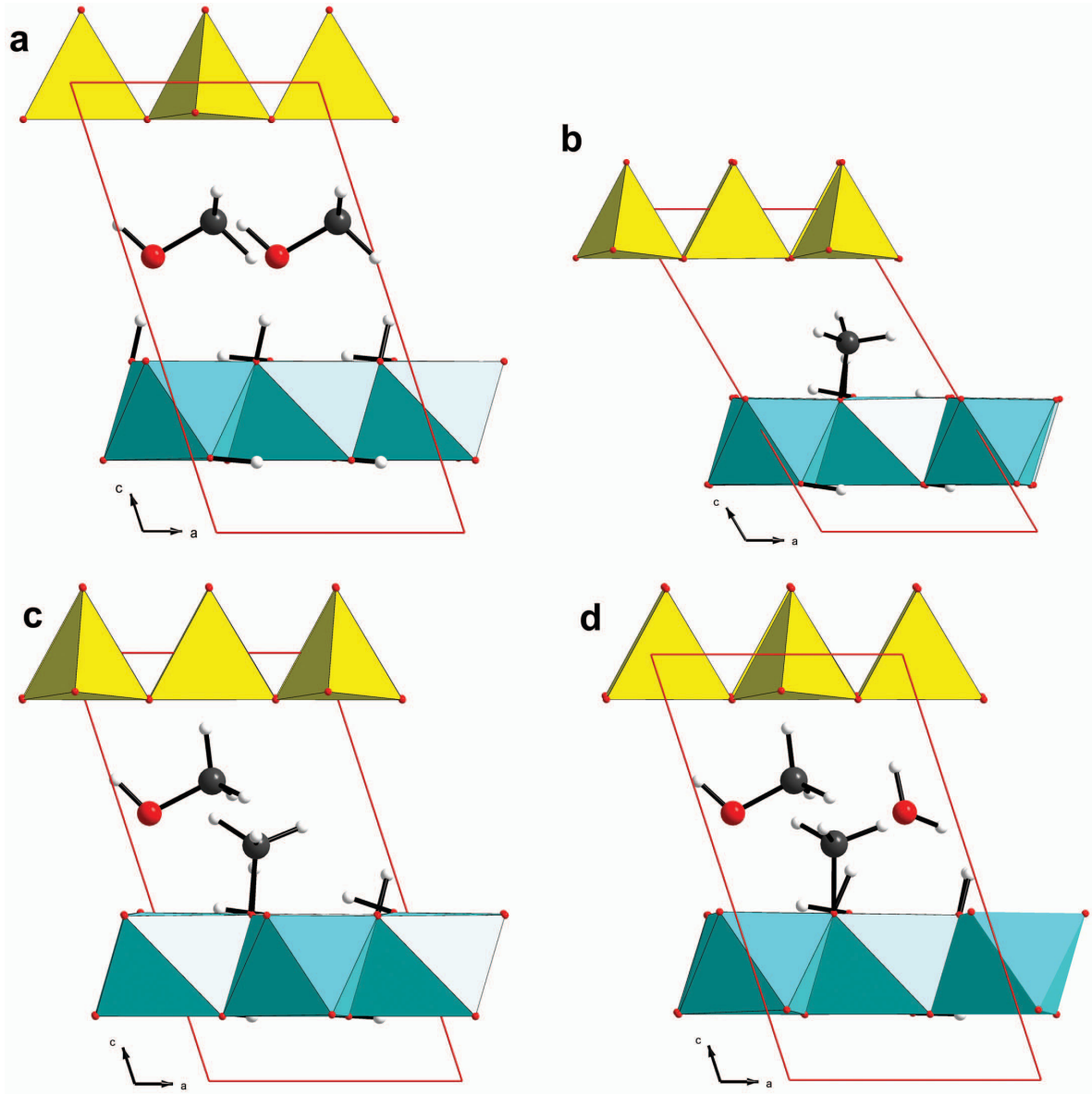

Figure 1. Structural models of the KM complex used for calculations: (a) K-INT, (b) K-MTX, (c) K-MIX, and (d) K-MIXW.

DMSO methyl groups. The ^{27}Al MAS NMR spectrum indicated a deformation of Al octahedra during DMSO intercalation as the signal was split into a peak with two maxima at: −10.1 and −24.9 ppm (Figure 4). The signal of pure kaolinite in the ^{29}Si MAS NMR (−91.0 ppm) was shifted to −92.3 ppm indicating a slight perturbation of the tetrahedral sheet (Figure 4).

The CHNS elemental analysis was used to estimate the chemical composition of the DMSO intercalate: $Al_2Si_2O_5(OH)_4(DMSO)_{0.65}$. The maximum molar amount which may be intercalated can be calculated by dividing the $Al_2Si_2O_5(OH)_4$ surface area (~23 Å^2, calculated from data published by Bish (1993)) by the DMSO cross-sectional area (~35 Å^2). The molar amount was 0.65, in very good agreement with the experimental data.

The reaction of the wet M40DS with methanol led to the formation of the KM complex in the experiments E1−E4. The d_{001} value of the new complex in all cases was ~11.2 Å (Figure 5), though the ID was relatively small (Table 2) and did not exceed 3% in E1 where the reaction was carried out at 50ºC. When the experiment was performed at room temperature and the methanol was not changed after each sample collection (E2), the ID reached only ~14%. The centrifugation and dispersion of the kaolinite in fresh methanol (E3) led to an increase of the ID to ~40% after 3.5 h. Increasing the time to 10 days (E4) did not improve the results much; the ID reached ~47%.

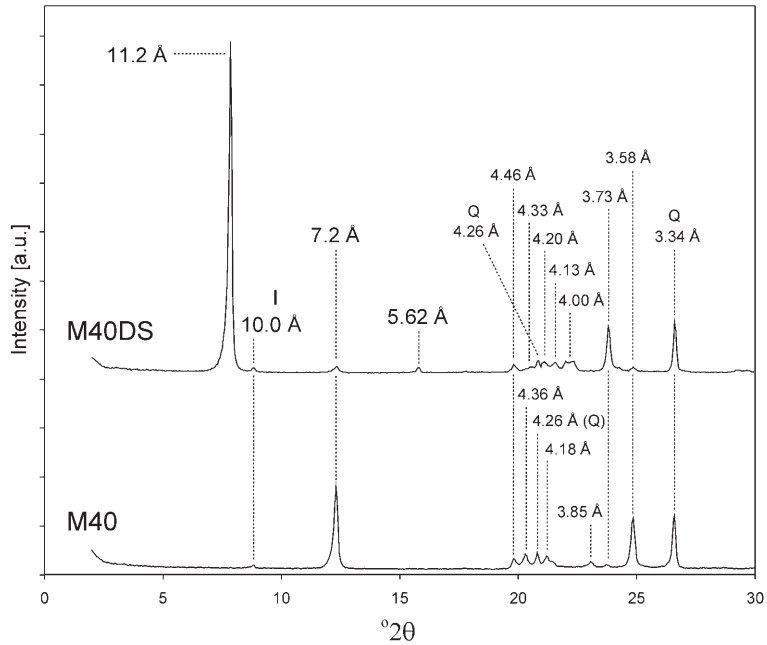

Figure 2. XRD patterns of: M40, raw kaolinite; M40DS, kaolinite after intercalation with DMSO. Abbreviations: I – illite, Q – quartz.

The IR spectra of the new complexes formed in the E1–E4 experiments (Figure 3) confirmed observations and assumptions based on the XRD data. In E1, after 1 h of reaction, DMSO molecules had been removed completely from the interlayer space and the characteristic spectrum of raw kaolinite was restored ($E1_{1.0\ h}D$ sample). High temperature did not improve the ID in this case. In E2 after 2 h of the reaction at room temperature ($E2_{2.0\ h}D$ sample), the presence of bands at 3539 and 3503 cm^{-1} (stretching modes of surface OH involved in hydrogen bonding between kaolinite and DMSO) indicated that DMSO was still in the kaolinite interlayer space. In E3 after 3.5 h ($E3_{3.5\ h}D$) and E4 after 10 days (data not shown), the spectrum was very similar and showed the presence of a broad band with maximum at 3430 cm^{-1} attributed to OH stretching of methanol molecules and/or to water molecules formed during the esterification reaction of kaolinite inner-surface OH groups and methanol molecules, respectively. Low-intensity C–H stretching bands were found at 2931 and 2860 cm^{-1}, and the OH-stretching bands were nearly identical to those of the pure kaolinite.

The results obtained in the E1–E4 procedures showed that the use of the M40DS which was not dried before the reaction with methanol reduced the efficiency of formation of the KM complex. The excess of very polar DMSO molecules effectively blocked the interlayer space and prevented the exchange of DMSO with methanol. Thus, the subsequent methanol intercalation and further grafting did not take place to a significant extent or these processes were considerably hampered.

Experiment 5 (dried M40DS)

The use of a M40DS complex which was previously dried at 70ºC for 24 h improved significantly the efficiency of formation of the KM complex. The XRD pattern of the sample collected after 1 day ($E5_{1\ d}$), recorded in a wet state, revealed a reflection with d = 11.2 Å (Figure 5). The ID was 98.1%. The XRD pattern of that sample did not change significantly in comparison to the XRD patterns of samples collected over the following days, confirming that drying of the M40DS prior to reaction with methanol was crucial for synthesizing the KM complex effectively. On the basis of the calculated ID, all layers, which were previously expanded with DMSO (ID = 98.2%), were intercalated with methanol (ID = 98.1%). As reported previously (Tunney and Detellier, 1996; Komori *et al.*, 2000; Matusik *et al.*, 2011a), drying of the complex led to removal of the intercalated methanol molecules and, therefore, the d value of the KM complex was reduced to 8.7 Å ($E5_{1\ d}D$ sample). Note that the intensity of the raw kaolinite reflection (7.2 Å) in the KM complex before ($E5_{1\ d}$ sample) and after drying ($E5_{1\ d}D$ sample) was nearly identical, indicating that drying removed only loosely bonded (intercalated) methanol molecules and did not lead to a partial collapse of the kaolinite interlayer space. In the $E5_{10\ d}$ sample two types of methanol molecules are suggested to have been present in the interlayer space in the wet state: (1) molecules grafted to an octahedral sheet in the form of a methoxy group (Al–O–C bond); and (2) mobile methanol and/or water molecules kept in the interlayer space *via* hydrogen bonds that can be removed partially during drying.

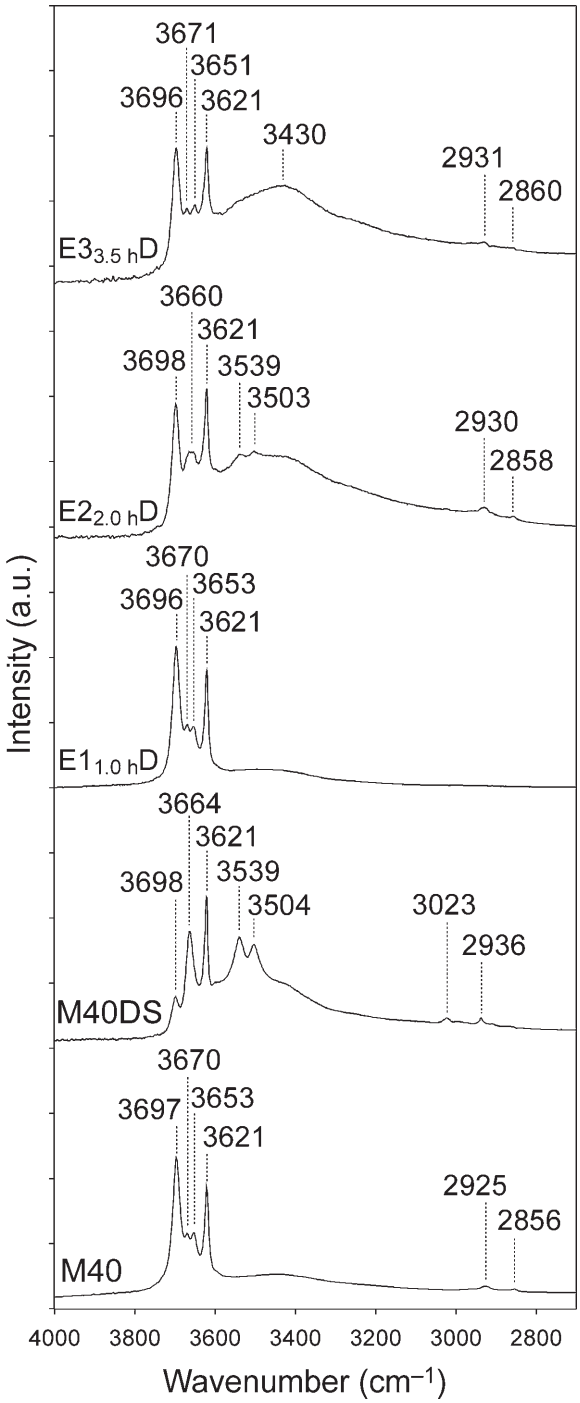

Figure 3. IR spectra of: M40, raw kaolinite; M40DS, kaolinite after intercalation with DMSO; E1$_{1.0\ h}$, E2$_{2.0\ h}$, E3$_{3.5\ h}$, M40DS after reaction with methanol in E1, E2, and E3, respectively. The subscript denotes time of reaction. D = dried.

The samples collected in the E5 experiment were dried at 120ºC and their IR spectra showed clearly that DMSO molecules were replaced by methanol after six washing cycles as the M40DS characteristic bands

Table 2. Changes in the degree of intercalation (ID) and d_{001} values during experiments (E1–E5).

Experiment	Sample/time	ID[a]	d_{001}
–	M40DS	98.2	11.2
E1	0.25 h	2.8	11.4
	0.5 h	2.5	11.4
	0.75 h	2.8	11.4
	1.0 h	2.2	11.4
E2	0.5 h	14.6	11.3
	1.0 h	14.5	11.3
	1.5 h	14.5	11.3
	2.0 h	14.1	11.3
E3	0.5 h	30.5	11.3
	1.0 h	30.2	11.3
	1.5 h	33.2	11.2
	2.0 h	31.4	11.2
	2.5 h	33.1	11.2
	3.0 h	35.9	11.2
	3.5 h	39.4	11.2
E4	1 d	43.4	11.2
	2 d	41.4	11.3
	3 d	47.5	11.2
	4 d	43.0	11.3
	5 d	45.0	11.3
	6 d	46.3	11.3
	7 d	46.8	11.3
	8 d	48.4	11.3
	9 d	49.4	11.3
	10 d	46.8	11.3
E5	1 d	98.1	11.2
	10 d	98.1	11.2

[a] ID = $I_{11}/(I_{11}+I_7)$*100%

(3542, 3506, 3022, and 2936 cm^{-1}) disappeared (Figure 6). On the other hand, CHNS elemental analysis indicated that sulfur content had already been reduced significantly after just two washing cycles (Figure 7). Nevertheless, sulfur traces were still present even after 10 washing cycles, indicating that a very small amount of the DMSO was still intercalated or adsorbed on the crystallite surfaces. The IR spectra showed changes in the intensity of the bands in the OH region due to intercalation and grafting of methanol (Figure 6). The local environment of inner-surface hydroxyl groups was altered significantly as new bands at 3646 and 3631 cm^{-1} appeared. The broad bands with maxima at 3564 and 3521 cm^{-1} may be related to loosely bonded methanol and/or water molecules. The bands in the C–H stretching region at 2954, 2920, and 2842 cm^{-1} confirmed the presence of $-OCH_3$ groups in the interlayer (Tunney and Detellier, 1996). Moreover, the intensity of the band assigned to interlamellar Al-OH groups (938 cm^{-1}) decreased significantly due to the formation of Al–O–C bonds (Figure 6). The presence of the methoxy groups (E5$_{10\ d}$D) was also confirmed by a

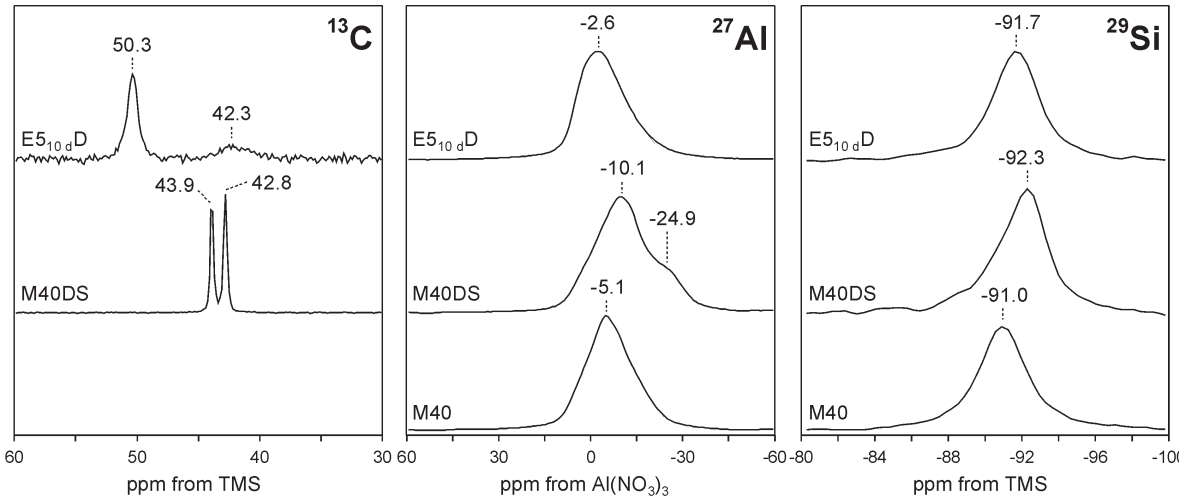

Figure 4. ^{13}C, ^{27}Al, and ^{29}Si spectra of: M40, raw kaolinite; M40DS, kaolinite after intercalation with DMSO; $E5_{10\ d}D$, dried kaolinite-methanol complex (E5).

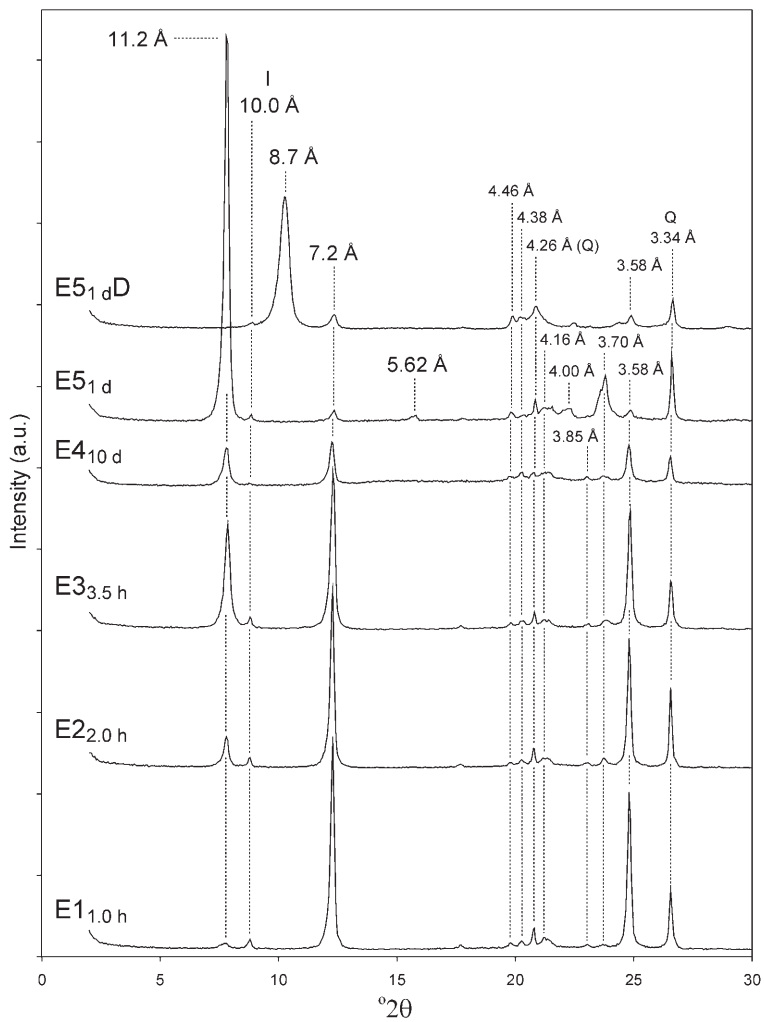

Figure 5. XRD patterns of M40DS after reaction with methanol in the experiments E1–E5. The subscript denotes the time of reaction. D = dried.

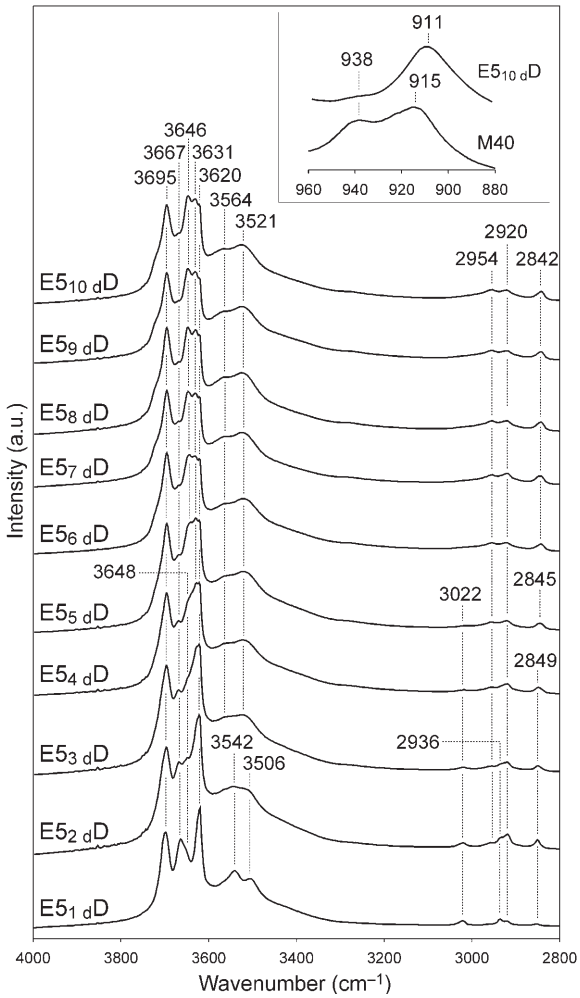

Figure 6. IR spectra of M40DS after reaction with methanol in E5. The subscript denotes the time of reaction. All samples were dried at 120ºC. The inset shows the spectra of M40 and E5$_{10\ d}$D in the 960−880 cm^{-1} region (Al-OH vibrations).

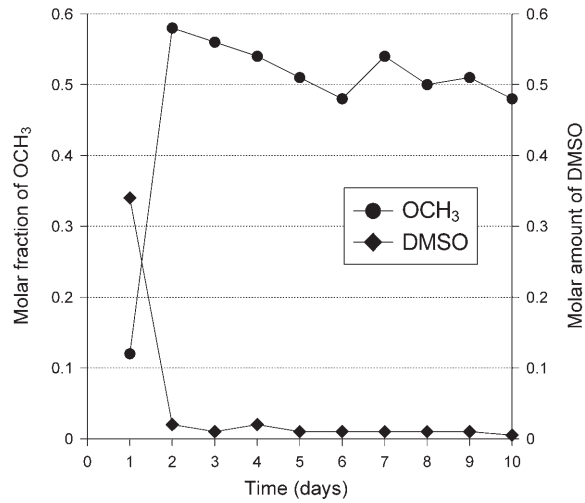

Figure 7. Variability of the amount of grafted -OCH$_3$ groups and amount of DMSO in E5 with time (based on the CHNS analyses).

resonance observed at 50.3 ppm in the ^{13}C CP-MAS NMR spectrum (Figure 4). The resonance at 42.3 ppm may have been related to the presence of a trace amount of the DMSO also indicated by the CHNS analysis. The washing of the M40DS sample with methanol led to a relaxation of the previously distorted Al-octahedra as a broad resonance with two maxima in the ^{27}Al MAS NMR spectrum was replaced by an asymmetric signal with chemical shift at −2.6 ppm (Figure 4). This signal was shifted slightly compared to the pure kaolinite. Thus, the grafting of methoxy groups did not affect the structure of the octahedral sheet significantly as was observed for a kaolinite grafted with ethylene glycol (Hirsemann *et al.*, 2011) probably because of the smaller molecular mass of the −CH$_3$ group compared to that of −CH$_2$−CH$_2$OH. The structure of the tetrahedral sheet was not affected by grafting as the chemical shift in the ^{29}Si MAS NMR spectra was close to that of the pure kaolinite (−91.0 ppm) and equal to −91.7 ppm. Assuming that all carbon was related to the methoxy groups formed, the chemical composition of the E5$_{10\ d}$D sample was estimated, on the basis of CHNS elemental analysis, to be $Al_2Si_2O_5(OH)_{3.52}(OCH_3)_{0.48}$, indicating that ~⅛ of the inner surface OH was grafted. The methoxy group content was >0.36 molecules per formula unit (m.p.f.u.) as reported by Komori *et al.* (2000) in an experiment performed under similar conditions. Tunney and Detellier (1996) synthesized a KM with a methoxy group content of 0.87 m.p.f.u. at temperatures of >200ºC. The E5$_{10\ d}$D sample was stirred in water for 24 h and dried at 120ºC to examine the grafting efficiency (Letaief and Detellier, 2007). After such treatment the d_{001} reflection was shifted slightly to ~8.5 Å indicating successful grafting of methoxy groups, while the intensity of the C−H stretching bands in the IR spectrum decreased due to removal of intercalated methanol and/or water (data not shown).

COMPUTATIONAL SIMULATION

Firstly, the DFT-D2 method was applied to the structure of pure kaolinite in order to reproduce the experimental data, especially the d_{001} distance. The data of Neder *et al.* (1999) were taken as a reference. The optimized cell parameters (a = 5.173 Å, b = 8.982 Å, c = 7.314 Å, α = 92.027º, β =105.207º, γ = 89.818º) were in very good agreement with the experimental data (see the section on computational models). The same was also found for the bond lengths where the differences were only in hundredths or thousandths of Å. The bond angles differed by a maximum of 3º. The

optimized d_{001} (7.06 Å) parameter agreed well with the experimentally obtained value of 7.15 Å (Neder *et al.*, 1999). The DFT-D2 approach was, therefore, concluded as being suitable for study of the KM complexes.

Complete optimization of the geometry (including unit cell) was performed for all four of the structural models described in the section on computational models. The largest d_{001} value of 9.4 Å was obtained for the model with two intercalated methanol molecules (K-INT, Figure 1a), while the smallest (7.7 Å) was found for the model with one grafted methoxy group (K-MTX, Figure 1b). X-ray diffraction measurements (Table 3) indicated that the K-MIX and K-MIXW models had d_{001} values closest to the experimental value observed for the $E5_{10\ d}D$ sample. The broad band below 3600 cm^{-1} in the measured IR spectrum of the $E5_{10\ d}D$ sample indicated the presence of water (Figure 8). The water was probably formed during an esterification reaction in the interlayer space. Based on this assumption, a detailed discussion of the theoretical IR spectrum of the K-MIXW model follows.

Table 3. Calculated d_{001} values of the KM complex models.

Model	d_{001} (Å)
K-INT	9.4
K-MTX	7.7
K-MIX	8.8
K-MIXW	9.1
$E5_{10\ d}D$ sample	8.7

Hydrogen bonds

Layers in kaolinite are held together *via* hydrogen bonds between adjacent layers linking a plane of surface hydroxyl groups of the octahedral sheet and basal oxygen atoms (O_b) of the tetrahedral sheet. In the pure kaolinite model the following structural characteristics were obtained: for the $O-H\cdots O_b$ bonds, the $H\cdots O_b$ distance is between 1.910 and 1.970 Å, the $O\cdots O_b$ distance is between 2.818 and 2.920 Å, and the $O-H\cdots O_b$ angle is between 157 and 165º. These parameters were typical for hydrogen bonds of moderate strength (Steiner, 2002; Desiraju and Steiner, 2006). Similar values were calculated in the work by Smrčok *et al.* (2010). Although in the K-MIXW model the hydrogen bonds became slightly weaker than in pure kaolinite, the additional moderate $O-H\cdots O$ and weak $C-H\cdots O$ hydrogen bonds (Castellano, 2004) contributed to the overall stability of the complex (Figure 9, Table 4). The methanol molecule was clearly keyed into the interlayer space through the multiple hydrogen bonds. The methoxy group was also stabilized by the $C_{mtx}-H_{mtx}\cdots O_b$ and $O_{is}-H_{is}\cdots O_{mtx}$ hydrogen bonds (mtx = methoxy, is = inner surface). The water molecule located in the interlayer space interacted with both the octahedral and tetrahedral sheet and completed a complex picture of the hydrogen-bond scheme in the K-MIXW model.

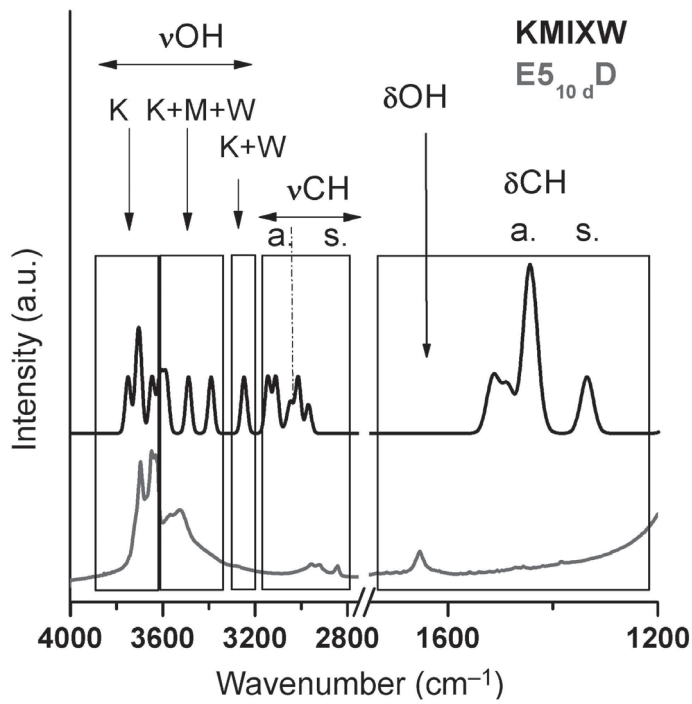

Figure 8. Comparison and analysis of calculated (K-MIXW model) and experimental ($E5_{10\ d}D$ sample) IR spectra.

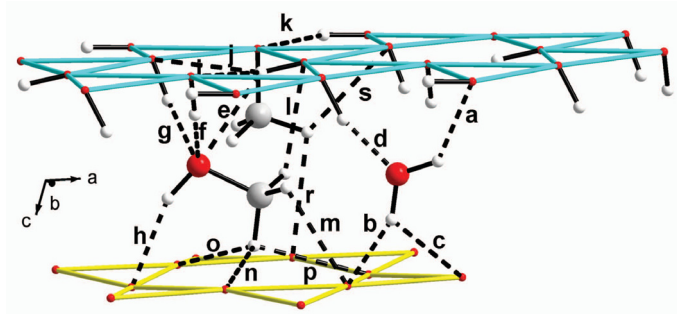

Figure 9. Hydrogen-bonds scheme of the K-MIXW model.

Vibrational analysis

Comparison of the calculated spectra of all models with the experimental spectrum of the $E5_{10\ d}D$ sample showed the best agreement for the K-MIXW model (Figure 10). Close attention was, therefore, paid to the 4000−1200 cm^{-1} region (Table 5) of the K-MIXW model spectrum, which can be divided into three parts (Figure 8).

The first part represented the OH-stretching vibrations (4000−3200 cm^{-1}). The highest-energy bands (4000−3640 cm^{-1}) were assigned to the stretching vibrations of the kaolinite OH groups. The bands with lower energy (3640−3380 cm^{-1}) corresponded to the stretching vibrations of the OH groups belonging to kaolinite, methanol, and water. The analysis confirmed the hypothesis that the broad bands with maxima at 3564 and 3521 cm^{-1} were related to loosely bonded methanol and/or water molecules. In this region, experimentally obtained bands corresponded to the OH-stretching vibrations of methanol (3612 cm^{-1}) and water (3587 cm^{-1}) in the calculated spectrum (Table 5). A complex band at 3249 cm^{-1} corresponded to the stretching vibrations of the OH groups of kaolinite and water (K+W). The second part of the spectrum (3150−2900 cm^{-1}) represented asymmetric (higher) and symmetric (lower) C−H stretching vibrations of the methanol and methoxy groups, respectively. The order of the stretching vibrations of the C−H groups in the K-MIXW model was: $\nu_{as}CH_{met} > \nu_{as}CH_{mtx} > \nu_{s}CH_{met} > \nu_{s}CH_{mtx}$ (Table 5). The third part of the spectrum (1700−1250 cm^{-1}) represented C−H bending vibrations of methanol and methoxy groups. Asymmetric bending vibrations had higher energy (1490−1460 cm^{-1}) than symmetric vibrations (1445−1335 cm^{-1}). In this region the bending vibration of the water was also found at 1514 cm^{-1}. The complete

Table 4. Hydrogen-bonds scheme in the interlayer space of the K-MIXW model (see Figure 9). Abbreviations: w − water, b − basal, met − methanol, mtx − methoxy, is − inner surface.

Symbol	Hydrogen bond	D−H (Å)	H···A (Å)	D...A (Å)	∠D−H···A (º)
a	$O_w-H_w\cdots O_{is}$	0.98	1.98	2.757	135
b	$O_w-H_w\cdots O_b$	0.97	1.87	2.680	139
c	$O_w-H_w\cdots O_b$	0.97	2.55	3.007	109
d	$O_{is}-H_{is}\cdots O_w$	0.99	1.65	2.608	159
e	$O_{is}-H_{is}\cdots O_{met}$	0.97	2.39	3.162	136
f	$O_{is}-H_{is}\cdots O_{met}$	0.99	1.73	2.694	163
g	$O_{is}-H_{is}\cdots O_{met}$	0.98	1.83	2.793	165
h	$O_{met}-H_{met}\cdots O_b$	0.98	2.03	2.952	157
i	$O_{is}-H_{is}\cdots O_{is}$	0.97	2.60	3.382	138
j	$O_{is}-H_{is}\cdots O_{is}$	0.97	2.57	3.344	136
k	$O_{is}-H_{is}\cdots O_{mtx}$	0.98	2.46	3.287	142
l	$C_{met}-H_{met}\cdots O_b$	1.09	2.45	2.992	109
m	$C_{met}-H_{met}\cdots O_b$	1.09	2.55	3.131	112
n	$C_{met}-H_{met}\cdots O_b$	1.09	2.49	2.948	104
o	$C_{met}-H_{met}\cdots O_b$	1.09	2.50	3.069	111
p	$C_{met}-H_{met}\cdots O_b$	1.09	2.62	3.003	100
r	$C_{mtx}-H_{mtx}\cdots O_b$	1.10	2.69	3.108	102
s	$C_{mtx}-H_{mtx}\cdots O_b$	1.10	2.60	3.199	114

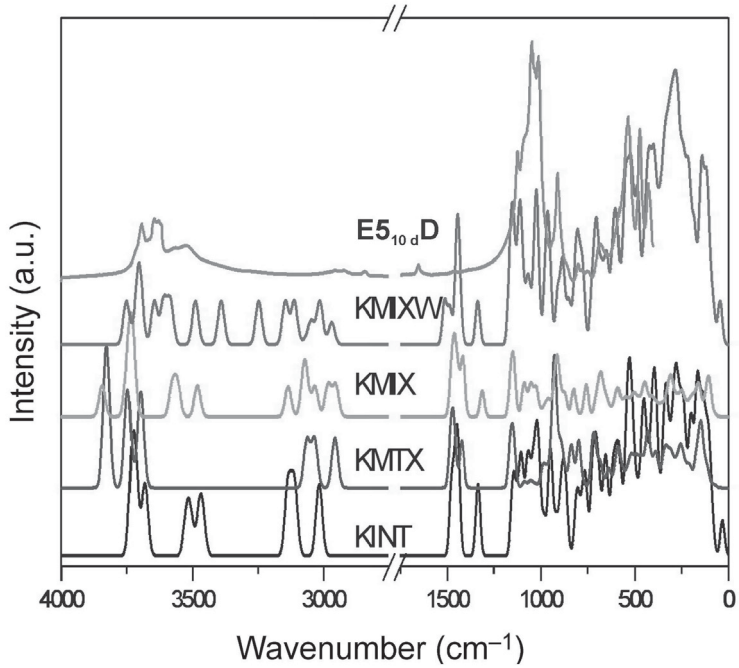

Figure 10. Calculated vibrational spectra of four structural models compared to the experimental IR spectrum of the E5$_{10\ d}$D sample.

assignment of the bands in the calculated spectrum of the K-MIXW model in the region above 1200 cm^{-1} and its comparison with the measured spectrum of the E5$_{10\ d}$D sample was shown in Table 5.

Table 5. Calculated wavenumbers of the K-MIXW model in the 4000−1200 cm^{-1} region. Abbreviations: w – water, b – basal, met – methanol, mtx – methoxy, is – inner surface.

Wavenumber (cm^{-1})	Type of vibration
3751	OH_{is} stretching
3711	OH_w stretching
3710	OH_{is}, OH_w stretching
3700	OH_i stretching
3648	OH_{is}, OH_w stretching
3612	OH_{met} , OH_{is} stretching
3587	OH_w, OH_{is}, OH_{met} stretching
3489	OH_{is}, OH_{met} stretching
3391	OH_{is}, OH_{met} stretching
3249	OH_{is}, OH_w stretching
3145	asym CH_{met} stretching
3111	asym CH_{met} stretching
3070	asym CH_{mtx} stretching
3048	asym CH_{mtx} stretching
3015	sym CH_{met} stretching
2969	sym CH_{mtx} stretching
1514	OH_w bending
1487	asym CH_{met}, CH_{mtx} bending
1453	asym CH_{met}, CH_{mtx} bending
1446	sym CH_{met}, CH_{mtx} bending
1444	sym CH_{met}, CH_{mtx} bending
1442	sym CH_{met}, CH_{mtx} bending
1428	sym CH_{mtx} bending
1335	HCO bending in methanol

CONCLUSIONS

The formation of the kaolinite-methanol complex (KM) was most effective at room temperature, when a dried kaolinite-dimethyl sulfoxide (KDS) precursor was used. The degree of intercalation reached ~98% after 24 h of stirring the KDS intercalation compound in methanol.

The CHNS elemental analysis showed that ~⅙ of the inner-surface OH groups were replaced by -OCH_3 methoxy groups. Traces of sulfur were detected even after 10 days of the KDS washing with methanol.

The exchange of DMSO molecules by methanol was less efficient when higher temperature was applied or wet KDS was used. The excess, highly polar DMSO molecules blocked the interlayer and prevented methanol intercalation and subsequent grafting.

The DFT-D2 method was used in order to support and interpret experimental observations of the grafted kaolinite. Four structural models of the KM complexes were proposed for this purpose. Analysis of the calculated structural parameters and computed IR spectra showed that the formation of hydrogen bonds was a key factor in the stabilization of the mixed grafted/intercalated KM complexes. Detailed analysis of the simulated IR spectra allowed assignment of bands to the particular vibrational modes and helped to interpret the measured IR spectra.

ACKNOWLEDGMENTS

This study was supported financially by the Ministry of Science and Higher Education within the "Iuventus Plus" research project No. IP2010 025070 (2010-2011). Eva Scholtzova is grateful for financial support from the Slovak Research and Development Agency (projects APVV 0362-10 and SK-AT-0020-10). Daniel Tunega acknowledges gratefully support by the German Research Foundation, the priority program SPP 1315, project GE/1676/1-1 and by the Austrian Agency for International Cooperation in Education and Research (OEAD), project SK 15/2011.

REFERENCES

Avila, L.R., de Faria, E.H., Ciuffi, K.J., Nassar, E.J., Calefi, P.S., Vicente, M.A., and Trujillano, R. (2010) New synthesis strategies for effective functionalization of kaolinite and saponite with silylating agents. *Journal of Colloid and Interface Science*, **341**, 186–193.

Benco, L., Tunega, D., Hafner, J., and Lischka, H. (2001a) Ab initio density functional theory applied to the structure and proton dynamics of clays. *Chemical Physics Letters*, **333**, 479–484.

Benco, L., Tunega, D., Hafner, J., and Lischka, H. (2001b) Orientation of OH groups in kaolinite and dickite. Ab initio molecular dynamics study. *American Mineralogist*, **86**, 1057–1065.

Benco, L., Tunega, D., Hafner, J., and Lischka, H. (2001c) Upper limit of the O–H...O hydrogen bond. Ab initio study of the kaolinite structure. *Journal of Physical Chemistry B*, **105**, 10812–10817.

Bish, D.L. (1993) Rietveld refinement of the kaolinite structure at 1.5 K. *Clays and Clay Minerals*, **41**, 738–744.

Blöchl, P.E. (1994) Projector augmented-wave method. *Physical Review B*, **50**, 17953–17979.

Bougeard, D., Smirnov, K.S., and Geidel, E. (2000) Vibrational spectra and structure of kaolinite: A computer simulation study. *Journal of Physical Chemistry B*, **104**, 9210–9217.

Castellano, R.K. (2004) Progress toward understanding the nature and function of C–H...O interactions. *Current Organic Chemistry*, **8**, 845–865.

de Faria, E.H., Lima, O.J., Ciuffi, K.J., Nassar, E.J., Vicente, M.A., Trujillano, R., and Calefi, P.S. (2009) Hybrid materials prepared by interlayer functionalization of kaolinite with pyridine-carboxylic acids. *Journal of Colloid and Interface Science*, **335**, 210–215.

Desiraju, G.R. and Steiner, T. (2006) *The Weak Hydrogen Bond: in Structural Chemistry and Biology*. Oxford University Press, New York.

Duer, M.J., Rocha, J., and Klinowski, J. (1992) Solid-state NMR studies of the molecular motion in the kaolinite: DMSO intercalate. *Journal of the American Chemical Society*, **114**, 6867–6874.

Farmer, V.C. and Russell, J.D. (1967) Infrared absorption spectrometry in clay studies. *Clays and Clay Minerals*, **15**, 121–142.

Fellah, M.F. (2011) Direct oxidation of methanol to formaldehyde by N_2O on $[Fe]^{1+}$ and $[FeO]^{1+}$ sites in Fe-ZSM-5 zeolite: A density functional theory study. *Journal of Catalysis*, **282**, 191–200.

Franco, F. and Ruiz Cruz, M.D. (2004) Factors influencing the intercalation degree ('reactivity') of kaolin minerals with potassium acetate, formamide, dimethylsulphoxide and hydrazine. *Clay Minerals*, **39**, 193–205.

Frost, R.L., Kristof, J., Horváth, E., and Kloprogge, J.T. (2000) Kaolinite hydroxyls in dimethylsulphoxide-intercalated kaolinites at 77 K – a Raman spectroscopic study. *Clay Minerals*, **35**, 443–454.

Gardolinski, J.E.F.C. and Lagaly, G. (2005) Grafted organic derivatives of kaolinite I. Synthesis, chemical and rheological characterization. *Clay Minerals*, **40**, 537–546.

Grimme, S., Antony, J., Schwabe, T., and Mück-Lichtenfeld, C. (2007) Density functional theory with dispersion corrections for supramolecular structures, aggregates, and complexes of (bio)organic molecules. *Organic & Biomolecular Chemistry*, **5**, 741–758.

Hayashi, S. (1997) NMR study of dynamics and evolution of guest molecules in a kaolinite/dimethyl sulfoxide intercalation compound. *Clays and Clay Minerals*, **45**, 724–732.

Hirsemann, D., Koster, T.K.J., Wack, J., van Wullen, L., Breu, J., and Senker, J.r. (2011) Covalent grafting to μ-hydroxy-capped surfaces? A kaolinite case study. *Chemistry of Materials*, **23**, 3152–3158.

Itagaki, T. and Kuroda, K. (2003) Organic modification of the interlayer surface of kaolinite with propanediols by transesterification. *Journal of Materials Chemistry*, **13**, 1064–1068.

Johnston, C.T. and Stone, D.A. (1990) Influence of hydrazine on the vibrational modes of kaolinite. *Clays and Clay Minerals*, **38**, 121–128.

Komori, Y., Sugahara, Y., and Kuroda, K. (1999) Intercalation of alkylamines and water into kaolinite with methanol kaolinite as an intermediate. *Applied Clay Science*, **15**, 241–252.

Komori, Y., Enoto, H., Takenawa, R., Hayashi, S., Sugahara, Y., and Kuroda, K. (2000) Modification of the interlayer surface of kaolinite with methoxy groups. *Langmuir*, **16**, 5506–5508.

Kresse, G. and Furthmüller, J. (1996a) Efficiency of ab-initio total energy calculations for metals and semiconductors using a plane-wave basis set. *Computational Materials Science*, **6**, 15–50.

Kresse, G. and Furthmüller, J. (1996b) Efficient iterative schemes for ab initio total-energy calculations using a plane-wave basis set. *Physical Review B*, **54**, 11169–11186.

Kresse, G. and Joubert, D. (1999) From ultrasoft pseudopotentials to the projector augmented-wave method. *Physical Review B*, **59**, 1758–1775.

Kuroda, Y., Ito, K., Itabashi, K., and Kuroda, K. (2011) One-step exfoliation of kaolinites and their transformation into nanoscrolls. *Langmuir*, **27**, 2028–2035.

Ledoux, R.L. and White, J.L. (1964) Infrared studies of the hydroxyl groups in intercalated kaolinite complexes. *Clays and Clay Minerals*, **13**, 289–315.

Letaief, S. and Detellier, C. (2007) Functionalized nanohybrid materials obtained from the interlayer grafting of aminoalcohols on kaolinite. *Chemical Communications*, **25**, 2613–2615.

Letaief, S., Tonle, I.K., Diaco, T., and Detellier, C. (2008) Nanohybrid materials from interlayer functionalization of kaolinite. Application to the electrochemical preconcentration of cyanide. *Applied Clay Science*, **42**, 95–101.

Li, Y., Sun, D., Pan, X., and Zhang, B. (2009) Kaolinite intercalation precursors. *Clays and Clay Minerals*, **57**, 779–786.

Machado, G.S., Groszewicz, P.B., Castro, K.A.D.F., Wypych, F., and Nakagaki, S. (2012) Catalysts for heterogeneous oxidation reaction based on metalloporphyrins immobilized on kaolinite modified with triethanolamine. *Journal of Colloid and Interface Science*, **374**, 278–286.

Matusik, J., Gaweł, A., Bielańska, E., Osuch, W., and Bahranowski, K. (2009) The effect of structural order on nanotubes derived from kaolin-group minerals. *Clays and Clay Minerals*, **57**, 452–464.

Matusik, J., Wisła-Walsh, E., Gaweł, A., Bielańska, E., and

Bahranowski, K. (2011a) Surface area and porosity of nanotubes obtained from kaolin minerals of different structural order. *Clays and Clay Minerals*, **59**, 116–135.

Matusik, J., Stodolak, E., and Bahranowski, K. (2011b) Synthesis of polylactide/clay composites using structurally different kaolinites and kaolinite nanotubes. *Applied Clay Science*, **51**, 102–109.

Matusik, J., Gaweł, A., and Bahranowski, K. (2012) Grafting of methanol in dickite and intercalation of hexylamine. *Applied Clay Science*, **56**, 63–67.

Michalková, A. and Tunega, D. (2007) Kaolinite: dimethylsulfoxide intercalate – a theoretical study. *Journal of Physical Chemistry C*, **111**, 11259–11266.

Michalková, A., Tunega, D., and Turi Nagy, L. (2002) Theoretical study of interactions of dickite and kaolinite with small organic molecules. *Journal of Molecular Structure (Theochem)*, **581**, 37–49.

Moretti, E., Storaro, L., Chessa, G., Talon, A., Callone, E., Mueller, K.J., Enrichi, F., and Lenarda, M. (2012) Stepwise dansyl grafting on the kaolinite interlayer surface. *Journal of Colloid and Interface Science*, **375**, 112–117.

Murakami, J. (2004) Synthesis of kaolinite-organic nanohybrids with butanediols. *Solid State Ionics*, **172**, 279–282.

Neder, R.B., Burghammer, M., Grasl, T.H., Schulz, H., Bram, A., and Fiedler, S. (1999) Refinement of the kaolinite structure from single-crystal synchrotron data. *Clays and Clay Minerals*, **47**, 487–494.

Olejnik, S., Aylmore, L.A.G., Posner, A.M., and Quirk, J.P. (1968) Infrared spectra of kaolin mineral-dimethyl sulfoxide complexes. *Journal of Physical Chemistry*, **72**, 241–249.

Perdew, J.P. and Wang, Y. (1992) Accurate and simple analytic representation of the electron-gas correlation energy. *Physical Review B*, **45**, 13244–13249.

Perdew, J.P. and Zunger, A. (1981) Self-interaction correction to density-functional approximations for many-electron systems. *Physical Review B*, **23**, 5048–5079.

Raupach, M., Barron, P.F., and Thompson, J.G. (1987) Nuclear magnetic resonance, infrared, and X-ray powder diffraction study of dimethylsulfoxide and dimethylselenoxide intercalates with kaolinite. *Clays and Clay Minerals*, **35**, 208–219.

Scholtzová, E. and Smrčok, Ľ. (2009) Hydrogen bonding and vibrational spectra in kaolinite-dimethylsulfoxide and -dimethylselenoxide intercalates – a solid-state computational study. *Clays and Clay Minerals*, **57**, 54–71.

Scholtzová, E., Benco, L., and Tunega, D. (2008) A model study of dickite intercalated with formamide and N-methylformamide. *Physics and Chemistry of Minerals*, **35**, 299–309.

Smrčok, Ľ., Tunega, D., Ramirez-Cuesta, A.J., and Scholtzová, E. (2010) The combined inelastic neutron scattering and solid state DFT study of hydrogen atoms dynamics in a highly ordered kaolinite. *Physics and Chemistry of Minerals*, **37**, 571–579.

Steiner, T. (2002) The hydrogen bond in the solid state. *Angewandte Chemie International Edition*, **41**, 48–76.

Tonle, I.K., Diaco, T., Ngameni, E., and Detellier, C. (2007) Nanohybrid kaolinite-based materials obtained from the interlayer grafting of 3-aminopropyltriethoxysilane and their potential use as electrochemical sensors. *Chemistry of Materials*, **19**, 6629–6636.

Tunney, J.J. and Detellier, C. (1993) Interlamellar covalent grafting of organic units on kaolinite. *Chemistry of Materials*, **5**, 747–748.

Tunney, J.J. and Detellier, C. (1996) Chemically modified kaolinite. Grafting of methoxy groups on the interlamellar aluminol surface of kaolinite. *Journal of Materials Chemistry*, **6**, 1679–1685.

Wada, K. (1961) Lattice expansion of kaolin minerals by treatment with potassium acetate. *American Mineralogist*, **46**, 78–91.

(*Received 14 February 2012; revised 6 April 2012; Ms. 653; A.E. J.W. Stucki*)